Chinese Chemical Letters 33 (2022) 2933–2936

Contents lists available at ScienceDirect

Chinese Chemical Letters

journal homepage: www.elsevier.com/locate/cclet

Enhancing the process of CO_2 reduction reaction by using CTAB to construct contact ion pair in Li-CO_2 battery

Shiyu Ma, Youcai Lu, Hongchang Yao, Qingchao Liu*, Zhongjun Li*

Green Catalysis Center, and College of Chemistry, Zhengzhou University, Zhengzhou 450001, China

ARTICLE INFO

Article history:
Received 8 August 2021
Revised 26 October 2021
Accepted 28 October 2021
Available online 5 November 2021

Keywords:
CO_2 reduction reaction
Li-CO_2 battery
Quaternary ammonium additive
Contact ion pair
AIMD

ABSTRACT

Aprotic Li-CO_2 batteries have attracted growing interest due to their high theoretical energy density and its ability to use green house gas CO_2 for energy storage. However, the poor ability of activating CO_2 in organic electrolyte often leads to the premature termination of CO_2 reduction reaction (CO_2RR) directly. Here in this work, cetyl trimethyl ammonium bromide (CTAB) was introduced into a dimethyl sulfoxide (DMSO) based Li-CO_2 battery for the first time to enhance the CO_2RR. Significantly improved electrochemical performances, including reduced discharge over-potential and increased discharge capacity, can be achieved with the addition of CTAB. *Ab initio* molecular dynamics (AIMD) simulations show that quaternary ammonium group CTA^+ can accelerate CO_2 reduction process by forming more stable contact ion pair (CIP) with CO_2^-, reducing the energy barrier for CO_2RR, thus improving the CO_2 reduction process. In addition, adding CTA^+ is also favorable for the solution-phase growth of discharge products because of the improved migration ability of stable CTA^+-CO_2^- CIP in the electrolyte, which is beneficial for improving the utilization ratio of cathode. This work could facilitate the development of CO_2RR by providing a novel understanding of CO_2RR mechanism in organic system.

The rapid increase in CO_2 emissions caused by the overuse of fossil fuel has resulted in many severe environmental issues [1]. Therefore, great efforts have been made to search for valuable use of CO_2, including the development of electrochemical and photochemical CO_2 reduction technologies [2,3]. Among them, energy storage devices such as Li metal based CO_2 batteries ($4Li^+ + 3CO_2 + 4e^- \leftrightarrow 2Li_2CO_3 + C$) have attracted increasing interest, which can operate with a high discharge potential (~2.8 V) and considerable theoretical energy density of 1876 Wh/kg [4–10], through the reduction of CO_2 in the discharge process.

With regard to Li-CO_2 batteries, the activation of CO_2 to form CO_2-related intermediate species is important to the discharge reaction. However, the existence of carbon-oxygen double bond makes the CO_2 molecule very stable and difficult to directly accept electron and reduce to $CO_2^{\bullet-}$ [10–15]. For example, CO_2 was initially proposed for use in Li-O_2 battery as a "gas assist" additive, in this case, O_2 is the electroactive species, and CO_2 can only reacts with reduced O_2 species by subsequent chemical reactions [16–18]. Recently, by *in situ* ambient pressure X-ray photoelectron spectroscopy, Wang *et al.* verified that pure CO_2 reduction is not electrochemically active at room temperature on porous carbon electrode in organic ionic liquid [19]. In order to activate CO_2 and promote CO_2 reduction kinetics, homogeneous liquid phase catalyst has been used. Yin *et al.* investigated the possibility of using quinones (Q) as liquid catalysts for CO_2 reduction in Li-CO_2 system [20]. Quinones were reduced at the cathode first to form Q^{2-}, then chemical reaction between Q^{2-} and CO_2 occurred to form quinone–CO_2 adducts, which were further reduced to discharge product. Slightly different from the activation mechanism of quinones, Khurram *et al.* employed an alkyl amine, 2-ethoxyethylamine (EEA) to react with CO_2 to form an EEA–CO_2 adduct by the formation of a N–C bond [9]. The EEA-CO_2 adduct is not only highly electroactive in the electrolyte, but that the N–C bond is selectively cleaved upon electron transfer, ultimately facilitating the conversion of CO_2 gas to Li_2CO_3. Except for the effect of catalyst molecules with high e^-/CO_2 affinity, in both of the two cases, Li^+ is also implicated in the formation process of the active adduct species, and enables crucial shift to discharge product.

Recently, Khurram *et al.* proposed that coupled e^-/Li^+ transfer can activate CO_2 to form the Li^+-CO_2^- intermediate, avoiding the formation of unstable CO_2^- radical only, and suggested that Li^+ can also form a contact ion pair (CIP) with CO_2-derived anion, facilitating the subsequent CO_2 reduction steps [21]. However, the amount of available Li^+ is usually limited because of the high desolvation energy of Li^+ in organic electrolyte (526.7 kJ/mol for dimethyl sul-

* Corresponding authors.
E-mail addresses: qcliu@zzu.edu.cn (Q. Liu), lizhongjun@zzu.edu.cn (Z. Li).

https://doi.org/10.1016/j.cclet.2021.10.089
1001-8417/

foxide, 494.9 kJ/mol for propylene carbonate and 385.0 kJ/mol for tetraethylene glycol dimethyl ether), thus the formation of Li^+-paired species in organic electrolyte is difficult, which leads to sluggish CO_2RR kinetics [21]. What is more, increasing the concentration of Li salt cannot enhance the availability of Li^+ due to the formation of solvent-sheathed CIP, in which Li^+ and anion are completely aggregated to form a fluid network [22]. Considering the factors above, adding an appropriate positive ion (M^+) with lower desolvation energy than that of Li^+ to couple an electron and assist the transfer of the electron to CO_2, may induce strong interactions between M^+ and CO_2 reduction intermediate in electrolyte, and therefore facilitate to achieve better CO_2 reduction kinetics.

In addition to reaction kinetics, cathode passivation caused by insulator discharge products is also a key factor that prevents the battery from achieving high energy density. It has been reported that the film-like discharge products produced by the surface growth pathway can hinder the conduction of electrons during the discharge process, resulting in passivation of the cathode, while the solution phase growth pathway can keep the cathode surface sufficiently exposed, so that the discharge process can continue, thus greatly improving the capacity of the battery. The reason why the solution phase growth pathway can be realized lies in the enhanced solubility and/or reactivity of discharge intermediate, which can be achieved by using soluble catalysts in electrolyte. In this regard, until now, few researches on the strategy to increase the capacity by regulating discharge paths have been explored in the Li-CO_2 battery. With these motivations, in this work, soft Lewis acid cetyl trimethyl ammonium bromide (CTAB, which structure was shown in Fig. S1 in Supporting information) with quaternary ammonium CTA^+ cation was introduced into a dimethyl sulfoxide (DMSO) based Li-CO_2 battery for the first time. The choice of long alkyl chain is based on the principle that the hydrophobic microenvironment can enhance the diffusion of CO_2 gas [23]. Additionally, the DMSO used in this system has a better ability to dissolve CO_2 [21,24]. With the CTAB additive, the Li-CO_2 battery can operate at high discharge current from 0.2 mA/cm^2 to 0.35 mA/cm^2 and displayed an excellent CO_2RR performance (a real discharge capacity up to 20 mAh/cm^2 at a current density of 0.2 mA/cm^2). A series of evidence have shown that the addition of CTAB greatly improves the dissolving ability of discharge intermediates, facilitating the formation of discharge product in the solution phase, which can alleviate the cathode passivation. *Ab initio* molecular dynamics (AIMD) simulations showed that the quaternary ammonium N^+ group can form more stable CIP with e^-/CO_2 in DMSO than Li^+, thus enhance the ability of activating CO_2 and improve the CO_2 reduction process.

Fig. 1a shows a typical configuration model of Li-CO_2 battery with CTAB additive, in which carbon paper (CP) was used as cathode and DMSO containing 1 mol/L $LiCF_3SO_3$ as the electrolyte. Fig. 1b displays the proposed discharge mechanism of CTA^+ assisted pathway of CO_2RR. With the existence of CTA^+, CO_2 is reduced by CTA^+/e^- pair to form CTA^+-CO_2^- CIP, and then reacts with Li^+ to produce Li_2CO_3 and C with the regeneration of CTA^+. The electrochemical performances of Li-CO_2 batteries with and without the addition of CTAB (20 mmol/L) were investigated. Fig. 1c presents the cyclic voltammograms (CVs) response of batteries at a constant scan rate of 0.1 mV/s. It can be clearly seen that the battery with CTAB exhibits a significantly higher reduction onset potential and a larger peak current density compared to the battery without CTAB, implying faster CO_2 reduction kinetics with the assistance of CTAB [20]. The discharge capacities of the batteries are given in Fig. 1d, which shows that with the addition of CTAB, a significantly increased discharge capacity of more than 20 mAh/cm^2 was achieved, while the battery without CTAB additive can only displayed a pitiful capacity of about 2 mAh/cm^2, at a current density of 0.2 mA/cm^2 with a discharge terminal voltage of 2.0 V. Additionally, even at higher current densities, batteries with CTAB addition still exhibit considerable discharge capacity (Fig. S2 in Supporting information), further confirmed the significantly improved CO_2RR performances with the addition of CTAB. The effect of the concentration of the added CTAB on the discharge capacity was also investigated. As shown in Fig. S3 (Supporting information), the discharge capacity was increased with increasing the concentration of CTAB from 2 mmol/L to 20 mmol/L, while decreased slightly when the concentration was raised to 30 mmol/L. The increase in discharge capacity is due to the more CTA^+ provided with increasing CTAB concentration [25,26], and the decrease of discharge capacity may be related to the reduced ion mobility of the cations and anions associated with CO_2RR caused by the high concentration of salt. In order to prove that the capacity of CTAB catalyzed Li-CO_2 battery comes from CO_2 reduction, rather than the side reaction in which CTAB participates, the battery is discharged in an Ar atmosphere and the results show that the capacity is pitiful (Fig. S4 in Supporting information). The results above showed that CTAB can facilitate the reduction reaction of CO_2, and significantly improve the electrochemical performances, including reduced discharge over-potential and increased discharge capacity. The influence of Br^- anion on the CO_2 reduction process can be ruled out by investigating the LiBr (20 mmol/L) added battery, the reason is concerned that the addition of LiBr does not improve the capacity of the battery (Fig. S5 in Supporting information). Br^- anion in CTAB can act as an effective oxidizing intermediator due to the generation of Br_2 which can chemical oxidize the discharge products [27], and the CTAB catalyzed battery exhibited a stable round-trip performance of 47 cycles, illustrating the potential application of CTAB for the rechargeable Li-CO_2 battery (Fig. S6 in Supporting information). The corresponding scanning electron microscope (SEM) images, X-ray diffraction (XRD) and Raman patterns of charged or cycled cathodes were shown in Figs. S7 and S8 (Supporting information), further verified the catalytic action of CTAB in charging process.

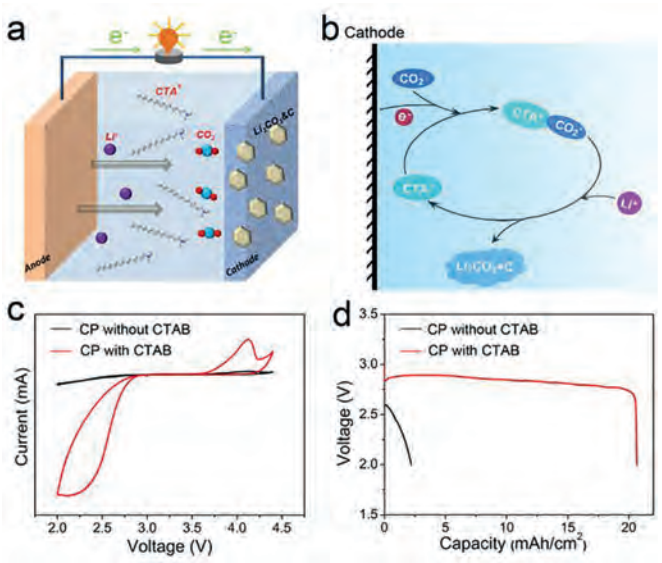

Fig. 1. (a) The typical configuration model of Li-CO_2 battery and (b) the proposed discharge mechanism catalyzed by CTAB. (c) CV curves of the batteries with and without CTAB additive. (d) Discharge capacities of the batteries with and without CTAB at a current density of 0.2 mA/cm^2.

To verify the morphology and distribution of the discharge products, deep discharged cathodes with and without CTAB additive were examined by SEM, respectively. Obviously, in the absence of CTAB, the CP surface is almost completely covered with fine particles of discharge products (Fig. 2a), leading to the cath-

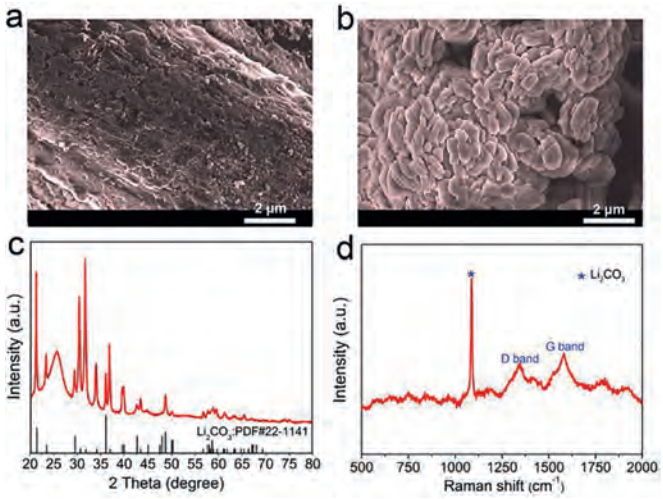

Fig. 2. SEM images of the cathode (a) without and (b) with CTAB additive after being deeply discharged at a current density of 0.2 mA/cm^2. (c) XRD pattern and (d) Raman spectrum of the discharged cathode with CTAB additive.

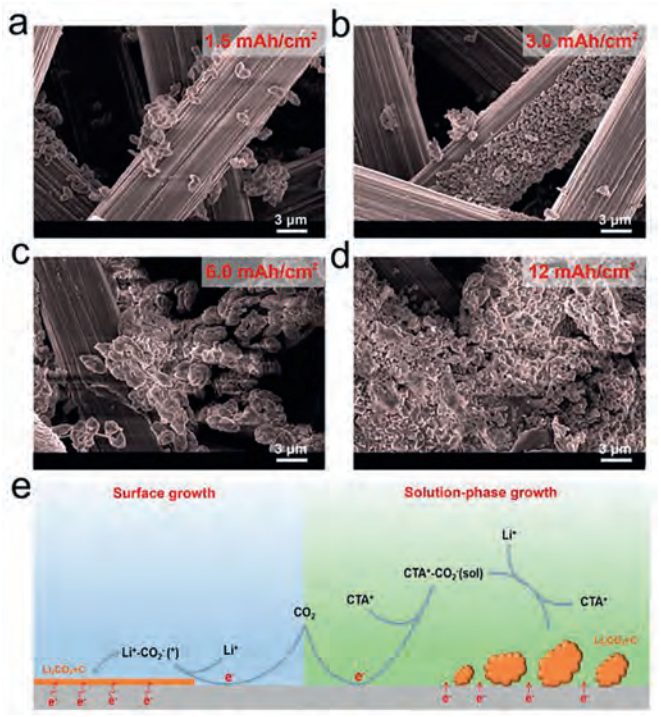

Fig. 3. SEM images of CTAB added cathode with capacity limited to (a) 1.5 mAh/cm^2, (b) 3.0 mAh/cm^2, (c) 6.0 mAh/cm^2 and (d) 12 mAh/cm^2, respectively. (e) Illustration of the different product growth pathways: surface and solution-phase growth.

ode passivation and poor CO_2RR kinetics of the battery. While vertical growth of large-size discharge products can be observed in the CTAB added battery, displaying a solution-phase growth pattern (Fig. 2b). To further illustrate this, the glass fiber separator in the deep discharged batteries with and without CTAB were also investigated as shown in Fig. S9 (Supporting information). For the battery without CTAB (Fig. S9a), the glass fiber is almost clean, while the glass fiber in the CTAB added battery was covered by foliated products (Fig. S9b), further demonstrated that the discharge products exhibit obvious solution-phase growth behavior, since the glass fiber is insulating. The XRD pattern and Raman shift spectroscopy were applied to investigate the discharge products in the CTAB added battery. As shown in Fig. 2c, the diffraction peaks at 21.2°, 30.5°, 31.6° can be assigned to the (110), ($\bar{2}$02), (002) planes of Li_2CO_3, respectively [6,28,29], and the characteristic Raman spectra peak at 1089 cm^{-1} is highly consistent with the standard patterns of Li_2CO_3 (Fig. 2d) [6], indicating the existence of Li_2CO_3 in the discharge products. To further confirm the component of discharge products in CTAB added Li-CO_2 batteries, sufficient HCl aqueous solution (1 mol/L) was used to remove Li_2CO_3. It can be found that the products presented a plate like morphology after being treated with HCl (Fig. S10 in Supporting information), which is characterized as carbon by Raman scattered spectrum (Fig. S11 in Supporting information), suggesting that the discharge products are Li_2CO_3 and C.

In order to further understand the effect of CTAB on the discharge process in Li-CO_2 battery, the evolution of discharge products in CTAB added battery was tracked at a current density of 0.2 mA/cm^2. As shown in Fig. 3, it can be seen that there are some aggregated and isolated discharge products formed after being discharged to 1.5 mAh/cm^2 (Fig. 3a), and the amount of which was increased with the discharge capacity raising from 1.5 mAh/cm^2 to 12 mAh/cm^2 (Figs. 3b–d). The characteristic of the formation of discharge products is that as the discharge process proceeds, large sized discharge products were continously aggregated on the cathode surface with a mode of expanding in both width and depth, avoiding the blocking of e$^-$ transfer channels on the cathode–electrolyte interface, which exhibits typical solution-phase growth behavior and is favorable to consecutive discharge process as well as the improvement of discharge capacity.

Based on the results above, the mechanisms of surface and solution-phase growth modes with and without CTAB are proposed and given in Fig. 3e, the formation and migration of M^+–CO_2^- CIP play the key role in the solution-phase growth of discharge products, in which the interaction of CTA^+ with CO_2^- is important to understanding the enhanced CO_2RR. In this regard, AIMD was used to investigate the structures and properties of the CIP formed by Li^+ and CTA^+ pair with CO_2^- in DMSO solvent, respectively. Representative snapshots of solvent-separated ion pair (SSIP) and CIP solvation models were shown in Figs. 4a–d. Each calculated solvent boxes contain DMSO solvent, three CO_2^- (CO_2 + e$^-$), and three simplified ammonium $CH_3CH_2(CH_3)_3N^+$ (denoted as N^+) or Li^+ ions. After 15 ps, it can be seen from Fig. 4b that three CO_2^- ions are almost all around an N^+ group, and the distance of CO_2^- from N^+ is 3.21, 3.379 and 4.9 Å, respectively, demonstrating that N^+ can easily contact with CO_2^-. However, only one CO_2^- is closed to the target Li^+ (the distance between them is 3.34 Å) (Fig. 4d), the strong solvation interaction between DMSO and Li^+ makes DMSO form a tight solvation shell around Li^+, hindering the contact of CO_2^- and Li^+. In contrast, N^+ can easily contact with CO_2^- and form more stable N^+-CO_2^- CIP than that of Li^+ due to the weak interaction between N^+ and DMSO. The energy barrier for the formation of the two CIP systems was further investigated as shown in Fig. 4e. Energy snapshots were conducted on four structures with an integration time-step of 1 fs during the AIMD time. It could be found that both the two CIP structures have lower energy over the entire AIMD time than their corresponding SSIP structures, confirming that the CIP structures are thermodynamically preferred in the electrolyte and isolated CO_2^- radicals are less likely to form alone. Obviously, the energy difference of N^+-CO_2^- CIP (–1.672 eV) is larger than that of Li^+-CO_2^- CIP (–0.893 eV), which indicates that N^+ can form stable CIP with CO_2^- easily. Therefore, according to the AIMD results above, it can be known that CTA^+ can enhance the CO_2 reduction kinetics by forming a more thermodynamically favorable CTA^+-CO_2^- CIP than Li^+-CO_2^- CIP. The former can combine with Li^+ in the electrolyte during its migration process to generate discharge products, enhancing the ability of forming products in the solution phase. The comparison of discharge

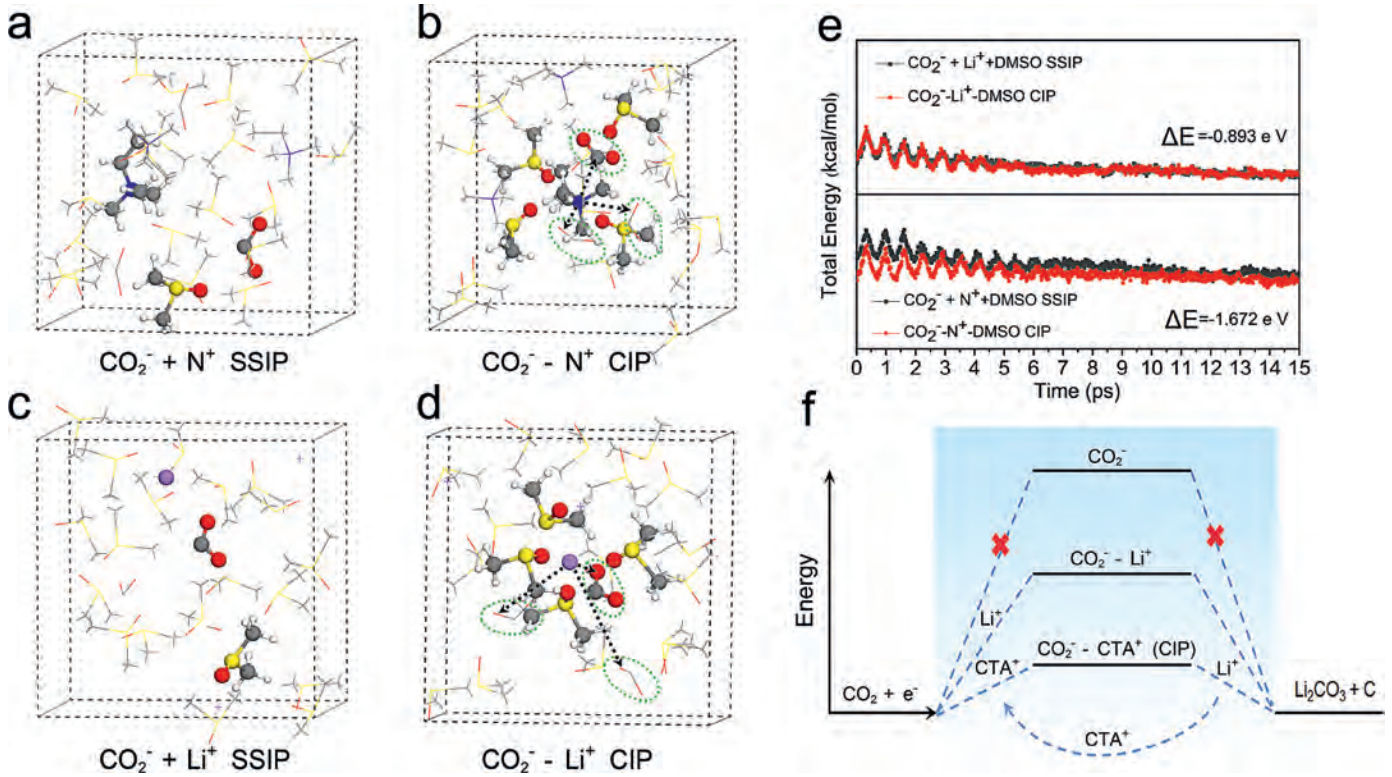

Fig. 4. Representative first solvation shell snapshots of SSIP and CIP models of (a, b) $CH_3CH_2(CH_3)_3N^+$ and (c, d) Li^+ with CO_2^- during the AIMD simulation, respectively (the contributed DMSO molecules are represented by a ball and stick model). Color code: C (gray), H (white), O (red), Li^+ (purple), N (blue), S (yellow), the green dotted ovals represent the other CO_2 molecules. (e) Average energies (0.5 ps) and total average energy differences (15 ps) of trajectories of SSIP and CIP. (f) Discharge pathways of Li-CO_2 batteries with and without CTA^+ based on the CIP energy profiles.

pathway of Li-CO_2 batteries with and without CTA^+ was shown in Fig. 4f, obviously, the different energy barrier for the formation of the two CIP systems changed the reaction pathway of CO_2 reduction, and the consequences of the CTA^+ catalyzed reaction route is the formation of stable CIP transfer, which dominates solution phase product formation and thus improves the discharge capacity of the battery.

In summary, in this work, CTAB was successfully introduced into Li-CO_2 battery system to greatly improve the electrochemical performances, including discharge over-potential and discharge capacity (a real discharge capacity can up to 20 mAh/cm^2 at a current density of 0.2 mA/cm^2 by using carbon paper cathode). Experiments coupled with AIMD showed that the CIP formed by CTA^+ and CO_2^- is more stable than that of Li^+ and CO_2^-, thus the CO_2 reduction process can be accelerated with the assistance of CTA^+. In addition, the introduced CTAB promotes the mobility of the discharge intermediates and makes the discharge products grow through the solution phase pathway, greatly eliminating the passivation of the cathode and finally releasing the battery energy. This work can facilitate the development of Li-CO_2 battery and provide a novel understanding of the CO_2 reduction chemistry in organic systems.

Declaration of competing interest

The authors declare that they have no known competing financial interests or personal relationships that could have appeared to influence the work reported in this paper.

Acknowledgments

This work is financially supported by National Science Foundation of China (Nos. 21701145 and 21701146), China Postdoctoral Science Foundation (Nos. 2017M610459 and 2018T110739).

Supplementary materials

Supplementary material associated with this article can be found, in the online version, at doi:10.1016/j.cclet.2021.10.089.

References

[1] T.F. Gao, A. Kumar, Z.C. Shang, et al., Chin. Chem. Lett. 30 (2019) 2274–2278.
[2] J.J. Sun, W.Z. Zheng, S.L. Lyu, et al., Chin. Chem. Lett. 31 (2020) 1415–1421.
[3] X.Y. Wang, J.F. Xie, M.A. Ghausi, et al., Adv. Mater. 31 (2019) 1807807.
[4] X. Xiao, P. Tan, X.B. Zhu, et al., ACS Sustain. Chem. Eng. 26 (2020) 9742–9750.
[5] B. Liu, Y.L. Sun, L.Y. Liu, et al., Energy Environ. Sci. 12 (2019) 887–922.
[6] Z.J. Xie, X. Zhang, Z. Zhang, Z. Zhou, Adv. Mater. 29 (2017) 1605891.
[7] Y. Qiao, J. Yi, S.C. Wu, et al., Joule 1 (2017) 359–370.
[8] X.W. Mu, H. Pan, P. He, H.S. Zhou, Adv. Mater. 32 (2019) 1903790.
[9] A. Khurram, M.F. He, B.M. Gallant, Joule 2 (2018) 2649–2666.
[10] S. Xu, S.K. Das, L.A. Archer, RSC Adv. 3 (2013) 6656–6660.
[11] Y. Xing, K. Wang, N. Li, et al., Matter 2 (2020) 1494–1508.
[12] E. Lamy, L. Nadjo, J.M. Saveant, J. Electroanal. Chem. 78 (1977) 403–407.
[13] C. Costentin, M. Robert, J.M. Saveant, Chem. Soc. Rev. 42 (2013) 2423–2436.
[14] J. Resasco, L.D. Chen, E. Clark, et al., J. Am. Chem. Soc. 139 (2017) 11277–11287.
[15] B. Gurkan, F. Simeon, T. A.Hatton, ACS Sustain. Chem. Eng. 3 (2015) 1394–1405.
[16] W. Yin, A. Grimaud, F. Lepoivre, et al., J. Phys. Chem. Lett. 8 (2017) 214–222.
[17] K. Takechi, T. Shiga, T. Asaoka, Chem. Commun. 47 (2011) 3463–3465.
[18] H.K. Lim, H.D. Lim, K.Y. Park, et al., J. Am. Chem. Soc. 135 (2013) 9733–9742.
[19] Y. Wang, W.W. Wang, J. Xie, et al., Nano Energy 83 (2021) 105830.
[20] W. Yin, A. Grimaud, I. Azcarate, et al., J. Phys. Chem. C 122 (2018) 6546–6554.
[21] A. Khurram, Y.M. Yin, L.F. Yan, et al., J. Phys. Chem. Lett. 10 (2019) 6679–6687.
[22] Y. Qiao, J. Yi, S.H. Guo, et al., Energy Environ. Sci. 11 (2018) 1211–1217.
[23] Z. Xing, L. Hu, D.S. Ripatti, et al., Nat. Commun. 12 (2021) 136.
[24] X. Li, S.X. Yang, N.N. Feng, et al., Chin. J. Catal. 37 (2016) 1016–1024.
[25] H. Wan, Y.J. Sun, Z.D. Li, et al., Energy Storage Mater. 40 (2021) 159–165.
[26] B. Gurkan, F. Simeon, T.A. Hatton, ACS Sustain. Chem. Eng. 3 (2015) 1394–1405.
[27] X.G. Wang, C. Wang, Z. Xie, et al., ChemElectroChem 4 (2017) 2145.
[28] Z. Zhang, Q. Zhang, Y.N. Chen, et al., Angew. Chem. Int. Ed. 54 (2015) 6550–6553.
[29] Z. Zhang, X.G. Wang, X. Zhang, et al., Adv. Sci. 5 (2018) 1700567.